(10) "International Tables for X-ray Crystallography", Vol. III, Kynoch Press, Birmingham, England, 1962, pp 202–211.
(11) R. F. Stewart, E. R. Davidson, and W. T. Simpson, *J. Chem. Phys.*, **42**, 3175 (1965).
(12) A. Vessieres, D. Touchard, and P. Dixneuf, *J. Organomet. Chem.*, **118**, 93 (1976).
(13) C. A. Tolman, *J. Am. Chem. Soc.*, **92**, 2956 (1970).
(14) R. Mason and A. I. M. Rae, *J. Chem. Soc. A*, 1767 (1970).
(15) T. Kashiwagi, N. Yasuoka, T. Ueki, N. Kasai, and M. Kakudo, *Bull. Chem. Soc. Jpn.*, **40**, 1998 (1967).
(16) A. H. Guenther, *J. Chem. Phys.*, **31**, 1095 (1959).
(17) B. Kleman, *Can. J. Phys.*, **41**, 2034 (1963).
(18) A. J. Carty, H. N. Paik, and G. J. Palenik, *Inorg. Chem.*, **16**, 300 (1977).
(19) F. A. Cotton and P. Lahuerta, *Inorg. Chem.*, **14**, 116 (1975).
(20) A. J. Carty, N. J. Taylor, and C. R. Jablonski, *Inorg. Chem.*, **15**, 1169 (1976).
(21) A. De Cian and R. Weiss, *Acta Crystallogr., Sect. B*, **28**, 3264 (1972).

(22) P. F. Lindley and O. S. Mills, *J. Chem. Soc. A*, 1279 (1969).
(23) Y. Wakatsuki, H. Yamazaki, and H. I. Wasaki, *J. Am. Chem. Soc.*, **95**, 5781 (1973).
(24) D. A. Allison, J. Clardy, and J. G. Verkade, *Inorg. Chem.*, **11**, 2804 (1972).
(25) B. T. Kilbourn, U. A. Raeburn, and D. J. Thompson, *J. Chem. Soc. A*, 1906 (1969).
(26) Force constants were calculated by the method of F. A. Cotton and C. S. Kraihanzel, *J. Am. Chem. Soc.*, **84**, 4432 (1962). Other values (mdyn Å⁻¹) not mentioned in the text are as follows: **2b**, 15.99; **2c**, 16.22; **2f**, 15.62; **2g**, 15.52; **3**, 15.58; **4**, 15.66; **5**, 15.79; **6**, 14.65.
(27) A. Reckziegel and M. Bigorgne, *J. Organomet.*, **3**, 341 (1965).
(28) T. A. Manuel and F. G. A. Stone, *J. Am. Chem. Soc.*, **82**, 366 (1960).
(29) H. L. Conder and M. Y. Darensbourg, *J. Organomet. Chem.*, **67**, 93 (1974).
(30) F. B. Ogilvie, J. M. Jenkins, and J. G. Verkade, *J. Am. Chem. Soc.*, **92**, 1916 (1970).

Contribution from Union Carbide Corporation, Chemicals and Plastics Division, South Charleston, West Virginia 25303

$[Rh_{17}(S)_2(CO)_{32}]^{3-}$. 1. An Example of Encapsulation of Chalcogen Atoms by Transition-Metal–Carbonyl Clusters

JOSÉ L. VIDAL,* R. A. FIATO, L. A. COSBY, and R. L. PRUETT

The reaction of a solution of $Rh(CO)_2acac$ and alkali carboxylates in a glyme solvent, with H_2S or SO_2 under ~ 300 atm of carbon monoxide and hydrogen at 140–160 °C, resulted in the isolation of $[C_6H_5CH_2N(C_2H_5)_3]_3[Rh_{17}(S)_2(CO)_{32}]$. The complex has been characterized via a complete three-dimensional X-ray diffraction study. The complex crystallizes in the primitive monoclinic space group $P2_1/n$, with $a = 14.990$ (2) Å, $b = 38.458$ (10) Å, $c = 16.206$ (3) Å, $\beta = 101.26$ (3)°, $V = 9163$ (1) Å³, and ρ (calcd) = 2.383 g cm⁻³ for mol wt 3286.83 and $Z = 4$. Diffraction data were collected with an Enraf-Nonius CAD 4 automated diffractometer using graphite-monochromatized Mo Kα radiation. The structure was solved by direct methods and refined by difference-Fourier and least-squares techniques. All nonhydrogen atoms have been located and refined; final discrepancy indices are $R_F = 5.0\%$ and $R_{wF} = 6.6\%$ for all 12 820 symmetry-independent reflections in the range $0° \leq 2\theta \leq 45°$. The structure consists of 16 rhodium atoms distributed in the corners of four stacked, parallel squares and of a S–Rh–S group located inside the cluster. Rhodium–rhodium bonding and nonbonding distances of 2.76–2.88 and ~ 3.40–3.60 Å, respectively, are found in the structure. The sulfur–rhodium lengths, 2.17 and 2.33 Å, are shorter than the sum of the covalent radii of the two elements. Average values for the terminal and bridging rhodium–carbon and carbon–oxygen lengths are in the ranges of 1.81–1.85 and 1.98–2.03 Å and 1.14–1.18 and 1.18–1.20 Å, respectively. The unusual chemical stability of $[Rh_{17}(S)_2(CO)_{32}]^{3-}$ is shown by its inertness to strongly basic or acidic conditions. The anion exhibits Brønsted acid–base chemistry consistent with

$$[Rh_{17}(S)_2(CO)_{32}]^{3-} \underset{2OH^-}{\overset{2H^+}{\rightleftharpoons}} \text{``}[Rh_{17}(S)_2(CO)_{32}H_2]^-\text{''}$$
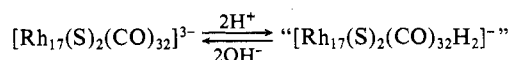
as indicated by infrared and elemental analysis. ¹³C solution NMR results are consistent with the solid-state structure indicating that it is maintained in solution. Some evidence is also presented which suggests that the anion is able to activate hydrogen at ambient conditions.

Introduction

Transition-metal–carbonyl clusters have attracted growing attention in the literature.[1–4] Much of this interest has been generated by the involvement of these compounds in a variety of catalytic reactions[3–16] and by the novel chemical behavior which they have exhibited.[3–19] Extra incentive for structural studies was provided by the opportunity offered for testing bonding theories.[1–3]

There are a number of examples of polynuclear metal clusters which contain isolated main-element atoms coordinated to the metal polyhedra. Isolated carbon atoms of the carbide type have been reported for systems in which this atom either is incompletely surrounded by metal atoms, as in $Fe_5(CO)_{15}C$,[20] or is completely coordinated to these atoms and placed inside the cavity of the metal polyhedra, as in $[Rh_6(CO)_{15}C]^{2-}$.[21] Further examples of transition-metal–carbonyl clusters containing coordinated main-element atoms in a fashion resembling that of $Fe_5(CO)_{15}C$ are provided for silicon ($[Co_4Si(CO)_{13}]$,[22]), for phosphorus ($[Co_4(\eta^5\text{-}C_5H_5)_4P_4]$[23]), for

arsenic ($[As_2(CO)_2(CO)_6]$[24]), and for sulfur, selenium, and tellurium ($[X_2Fe_3(CO)_9]$ (X = S, Se, Te)[25]).

Atomic sulfur is reported[26] to be a versatile ligand toward transition-metal complexes and the following modes of linkage are described: (1) a double-bridging, two-electron-donating ligand in $[Mo_2(\eta^5\text{-}C_5H_5)_2(O)_2(\mu\text{-}S)_2]$ and in $[Mo_3(\eta^5\text{-}C_5H_5)_3S_4]$; (2) a triply bridging, four-electron-donating, trigonal-pyramidal-like ligand in $[Co_3(CO)_9S]$, $[Co_3(\eta^5\text{-}C_5H_5)_3S_2]$, and $[Co_4(\eta^5\text{-}C_5H_5)_4S_4]$; (3) a quadruply bridging, four-electron-donating, square-pyramidal-like ligand in $[Co_4(CO)_{10}(S)_2]$; and (4) a quadruply bridging, six-electron-donating, tetrahedral-like ligand in $[Fe_2(CO)_6(\mu\text{-}SCH_3)]_2S\text{-}$ and in $[Re_2Mo(\eta^5\text{-}C_5H_5)(CO)_8]S[SMo(\eta^5\text{-}C_5H_5)(CO)_3]$. An in-depth study of these compounds has been done by Dahl's group.[23–33]

Other high-nuclearity transition-metal–carbonyl clusters have been found to encapsulate metal atoms, e.g., $[Rh_{13}(CO)_{24}H_{5-n}]^{n-}$,[12,34] and isolated carbon atoms, e.g., $[Rh_8(CO)_{19}C]$,[35] $[Rh_{12}(CO)_{25}(C)_2]$,[36] and $[Rh_{15}(CO)_{28}(C)_2]^-$.[37] In

contrast, examples of compounds in which an atom of group 5 or 6 is located inside of a cluster cavity have not been reported yet.

The ability of rhodium–carbonyl clusters to catalyze the formation of alcohols such as methanol and ethylene glycol, from carbon monoxide and hydrogen, the presence of sulfur-containing species such as SO_2 and H_2S in this important industrial feedstock, and the lack of reports concerning the reactions of rhodium–carbonyl clusters with sulfur-containing ligands provided impetus for the present study.

We describe in this paper the synthesis, structure, and some reactions of $[Rh_{17}(S)_2(CO)_{32}]^{3-}$. This anionic rhodium-carbonyl cluster provides the first examples of a transition-metal cluster with sulfur atoms located in the cavity of the cluster and of a rhodium–carbonyl cluster with an arrangement of metal atoms resembling the body-centered cubic packing of atoms present in some metals.

Experimental Section

Commercially available solvents, $Rh(CO)_2AcAc$, benzyltriethylammonium chloride, cesium benzoate, potassium hydroxide, phenylglyoxal dihydrate, and cesium hydroxide were used without additional treatment. Infrared spectra were taken in acetone solution and calibrated with polyethylene on a Beckman IR-12A spectrophotometer. Nuclear magnetic resonance ^1H and ^{13}C spectra were taken in acetone-d_6 solution (0.8 g of compound in 2.0 mL of solvent) on a Varian FT-XL-100 spectrometer. Proton NMR was studied in the range of δ 0 to -50, while ^{13}C spectra were studied up to 310 ppm downfield of tetramethylsilane used as external standard, using natural-abundance ^{13}C samples. Work was done in air without special protection from atmospheric contact unless otherwise noted. Analyses were done by Schwarzkopf Microanalytical Laboratory, Woodside, N.Y., and the single-crystal structure determination was conducted by Molecular Structure Corp., College Station, Texas.

Preparations of $[C_6H_5CH_2N(CH_2CH_3)_3]_3[Rh_{17}(S)_2(CO)_{32}]$ and $[Cs(C_{12}H_{24}O_6)_3]_3[Rh_{17}(S)_2(CO)_{32}]$. (a) $Rh(CO)_2acac$ (12.0 g, 46.3 mmol) was dissolved in 500 mL of tetraethylene glycol dimethyl ether containing cesium benzoate (2.42 g, 9.53 mmol) previously dissolved in several drops of water or methanol. H_2S or SO_2 (6.05 mmol) was measured in a vacuum line and condensed into an evacuated round-bottom flask containing 500 mL of solvent. Both solutions were mixed and the resulting mixture was charged to a previously evacuated high-pressure autoclave, which was then pressurized to 300 atm with a 1:1 mixture of carbon monoxide and hydrogen previously prepared in a gas-mixing autoclave. The system was heated to 160–180 °C and maintained under those conditions overnight.

The final solution was collected into a 1500-mL nitrogen-purged Schlenk receiver and filtered to remove any insoluble residue. The filtrate was treated with benzene (12:1 ratio) and allowed to stand overnight. The oil left after solvent decantation was redissolved in 2-propanol. This alcoholic solution was column chromatographed with silica gel and treated with a similar volume of a 2-propanol solution of benzyltriethylammonium chloride (1.0 g for every 15.0 mL). The red-violet solid precipitate (6.52 g) was collected by filtration and washed on the filter with fresh 2-propanol (5 × 10 mL); yield 72.8%.

The product was redissolved in acetone. The filtrate was treated with 2-propanol used as cosolvent, and crystals were grown by the slow-diffusion method. Anal. Calcd for $C_{71}H_{66}N_3O_{32}S_2Rh_{17}$: C, 25.92; H, 2.02; N, 1.28; S, 1.95; Rh, 53.26. Found: C, 25.98; H, 2.05; N, 1.47; S, 2.05; Rh, 53.15.

(b) $[Cs(C_{12}H_{22}O_6)_2]^+$ salt was prepared by a similar procedure but the resulting tetraglyme solution was added to an equivalent volume of a 1:1 volume mixture of water and 18-crown-6. The violet-red solid collected by filtration was washed with an excess of fresh, cold water and with 2-propanol. The product (4.32 g) was vacuum-dried and used in other studies. Anal. Calcd for $C_{104}H_{132}O_{68}Cs_3S_2Rh_{17}$: C, 26.6; H, 3.09; Cs, 8.49; S, 1.37; Rh, 37.26. Found: C, 30.96; H, 3.09; Cs, 8.07; S, 0.94; Rh, 37.54.

Preparation of "$[Rh_{17}(CO)_{32}(S)_2]Cs H_2 \cdot n(18\text{-crown-}6)$". A sample of 4.0 g of $[Rh_{17}(S)_2(CO)_{32}]Cs_3 \cdot 6(18\text{-crown-}6)$ was dissolved in 15 mL of acetone at 25 °C under carbon monoxide. A 1.0-mL aliquot of ca. 60% H_2SO_4 was then added and the solution stirred at room temperature for 30 min. The solution was then concentrated to ca.

6-mL total volume at 30–40 mm. The solid which precipitated was collected by filtration, redissolved in 15 mL of acetone, and treated once again with 1.0 mL of 60% aqueous H_2SO_4. The solution was then concentrated under vacuum (30–40 mm) and the resulting solid collected by filtration. The sample was then dried under vacuum (40–50 °C ($\sim$2–3 mm)). The solid that remained, 2.2–2.4 g, was quite soluble in acetone; IR (cm^{-1}) 2025, 1875, 1845. Elemental analysis indicated that the material had ca. 25–30% of the Cs:Rh level that was present in the starting sulfide complex.

This material can be reacted with NH_4OH or KOH which resulted in the replacement of H^+ with NH_4^+ or K^+, respectively.

Hydrogenation of Phenylglyoxal Dihydrate. Phenylglyoxal dihydrate (2.5 g, 14.88 mmol) was dissolved in 25 mL of freshly distilled tetrahydrofuran and $[Cs(C_{12}H_{24}O_6)_n]_3[Rh_{17}(S)_2(CO)_{32}]$ (0.250 g, 0.071 mmol based on rhodium) was added to the magnetically stirred solution. A stream of hydrogen was passed into the system at room temperature for 150 h. The solution was inspected visually during that period, and by filtration at the end of it, it was concluded that insoluble products were absent. The infrared spectrum of the solution showed the presence of the initial anion as the only metal–carbonyl species detectable. Separation of the final mixture by column chromatography on a Chromosorb 10 column resulted in the isolation of the major component of the mixture (0.51 g). This material was characterized by mass and nuclear magnetic resonance spectroscopy as $C_6H_5C(OH)HCH_3$; yield 28.1%.

X-ray Data Collection and Reduction. A black prismatic crystal with dimensions 0.15 × 0.15 × 0.35 mm was selected for the study. It was mounted on the tip of a thin glass fiber which was then inserted into a 0.2 mm diameter glass capillary. The capillary was then flame-sealed and seated into a pin on an eucentric goniometer. All crystal manipulations were done under argon. The goniometer was mounted on an Enraf-Nonius CAD4 automated diffractometer under the control of a PDP 11/45 computer.

The diffractometer was equipped with a molybdenum X-ray tube [λ(Mo Kα) 0.710 73 Å], operated at 50 kV and 21 mA, and with a graphite-crystal incident-beam monochromator. The crystal was centered in a random orientation. A counter aperture width of 2.0 mm, a crystal-to-detector distance of 21 cm, and an incident-beam collimator diameter of 2.0 mm were used during the study.

Intensity data was now collected via a θ(crystal)–2θ(counter) scan. The scan was done from $[2\theta(\text{Mo K}\alpha_1) - 0.6]°$ to $[2\theta(\text{Mo K}\alpha_2) + 0.6]°$. The variable scan rate used allows rapid data collection for intense reflections where a fast scan rate is used and ensures good counting statistics for weak reflections where a slow scan rate is used. Stationary-crystal, stationary-counter background counts (B_1 and B_2) were taken both at the beginning and at the end of the scan, each for half the time of the scan; this obviously resulted in a ratio (R) of scan time to background counting time of 2.0. The stability of the system was monitored by measuring three strong representative reflections periodically. No significant changes were found. The net intensity (I) and its standard deviation ($\sigma(I)$) were calculated from

$$I = S(C - RB)$$

$$\sigma(I) = [S^2(C + R^2B) + p^2]^{1/2}$$

where S is the scan rate, C is the total integrated peak, R is the ratio of the scan time to background counting time, and p, an ignorance factor introduced to downweight intense reflections, was set to 0.05. Any negative value of I was reset to zero. A reflection was considered to be statistically observed if the integrated intensity, I, was greater than twice the esd, $\sigma(I)$, of the intensity. It was not necessary to apply to the data corrections for changes in the intensity of the standard reflections, nor absorption corrections, since extinction was not observed or refined. No absorption correction was necessary because of the small linear absorption, $\mu = 30.01$ cm^{-1}. Lorentz and polarization corrections were applied to the data as needed.

An examination of the complete set of intensity data revealed the systematic absences of $0k0$ for $k \neq 2n$ and $h0l$ for $h + l \neq 2n$, consistent with the monoclinic space group $P2_1/n$. The systematically absent reflections were rejected.

Numerical information on data collection is given in Table I.

Solution and Refinement of the Structure. Computer programs used were those of the Enraf-Nonius Structure Determination Package on the PDP 11/45 computer system at the Molecular Structure Corp., College Station, Texas, using the programs written chiefly by Okaya and Frenz.

Table I. Data for the X-ray Diffraction Study of
$[C_6H_5CH_2N(C_2H_5)_3]_3[Rh_{17}(S)_2(CO)_{32}]$

(A) Crystal Data

crystal system: monoclinic	$\alpha = \gamma = 90.0$ (1)°
space group: $P2_1/n$	$\beta = 101.26$ (2)°
$a = 14.990$ (2) Å^a	$V = 9163$ (1)° Å^3
$b = 38.458$ (10) Å	$T = 23 \pm 1$ °C
$c = 16.206$ (3) Å	$Z = 4$
	ρ(calcd) = 2.383 g cm^{-3}

(B) Intensity Data

radiation: Mo Kα ($\bar{\lambda}$ 0.710 73 Å)
monochromator: graphite-crystal incident-beam
reflections measd: $+h, +k, +l$
take-off angle: 5.0°
max 2θ: 45°
min 2θ: 0°
scan type: θ–2θ
scan speed: 4–20°/min
scan range: symmetrical, $[2\theta(\text{Mo K}\alpha_1) - 0.6]°$ to
 $[2\theta(\text{Mo K}\alpha_2) + 0.6]°$
reflections collected: 13 057 total, 12 820 independent
max dev of std reflections: did not vary greater than
 normal changes in counting statistics
absorption coeff: 30.01 cm^{-1}; no absorption
 correction made
$F(000)$: 6264

^{a} Cell constants were obtained by computer-centering of
25 reflections, followed by least-squares refinement of the
setting angles.

Scattering factors were taken from Cromer and Waber.[38] The anomalous dispersion effects were included in F_c; both the real ($\Delta f'$) and imaginary ($\Delta f''$) components of anomalous dispersion for all the nonhydrogen atoms were those of Cromer and Lieberman.[39]

The function minimized during least-squares refinement was $\sum w(|F_o| - |F_c|)^2$ where the weight w is defined as $4F_o^2/\sigma^2(F_o^2)$. Discrepancy indices used in this work are defined by eq 1 and 2.

$$R_F = \sum ||F_o| - |F_c||/\sum |F_o| \qquad (1)$$

$$R_{wF} = [\sum w(|F_o| - |F_c|)^2/\sum wF_o^2]^{1/2} \qquad (2)$$

The structure was solvated by direct methods. A total of 16 phase sets were produced using 379 reflections with $|E_{\min}|$ of 2.40 and 2000 phase relationships. A chemically sensible "E" map from which the positions of the 17 rhodium and two sulfur atoms could be quickly ascertained was prepared from the phase set showing the first best-probability statistics (absolute figure of merit = 1.0042, residual, 28.94). These atoms were included in least-squares refinement leading after two cycles of full-matrix least-squares refinement to positional and isotropic thermal parameters with R_F = 21% and R_{wF} = 29%. Succeeding difference-Fourier syntheses then led to the unambiguous location of all the remaining nonhydrogen atoms. The 17 rhodium and the two sulfur atoms were refined anisotropically, while the remaining carbon, oxygen, and nitrogen atoms were refined isotropically.

Only 5980 reflections having $F_o^2 > 3\sigma(F_o^2)$ were used in continuing the analysis. Refinement of the positional and anisotropic thermal parameters for all nonhydrogen atoms led to convergence with R_F = 5.0% and R_{wF} = 6.6%. For the 125 atoms studied, the number of variable parameters considered was 428 for the anion and 169 for the cation. The esd of an observation of unit weight was then 1.606, while the maximum parameter shift was 0.7 times its esd.

The function $\sum_w(|F_o| - |F_c|)^2$ showed no unusual trends or appreciable dependence upon $\lambda^{-1} \sin \theta$, or upon $|F_o|$, as shown by plots of the above function vs. $|F_o|$ and $\lambda^{-1} \sin \theta$. Similar conclusions could be drawn about the dependence of this function with the reflection order in data collection. Thus, the weighting scheme is acceptable. There was no evidence for secondary extinction. The final difference-Fourier map showed no residual electron density as high as carbon atoms on a previous difference-Fourier map.

Positional parameters are included in Table II. Complete tables of observed and calculated structure factor amplitudes, thermal parameters, and bond lengths and bond angles are available as supplementary material.
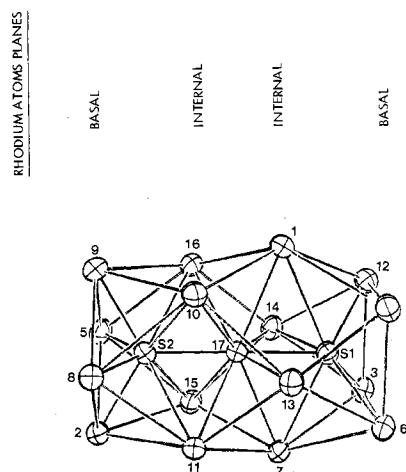
Figure 1. ORTEP diagram of $[Rh_{17}(S)_2(CO)_{32}]^{3-}$ with the carbon monoxide ligands omitted.

Results and Discussion

The crystal structure consists of discrete $[Rh_{17}(S)_2(CO)_{32}]^{3-}$ anions and $[C_6H_5CH_2N(C_2H_5)_3]^+$ cations separated by van der Waals contacts. A view of the trianion, in which the carbon monoxide ligands have been eliminated for easier interpretation, is shown in Figure 1.

Description of the Structure. A description of the structure of the cluster may be required in view of its apparent complexity. Sixteen rhodium atoms are defining the cluster's skeleton. These atoms are distributed in the corners of four stacked parallel squares, which are staggered by 45°. The geometric center of each of the squares is located on the C_4-symmetry axis defined by the S–Rh–S group located in the cluster cavity. Thus, the basic rhodium core of the cluster consists of two basal or "external" rhodium planes and two other rhodium planes in a relative internal position along the cluster longitudinal axis. Each of the rhodium atoms placed on the basal planes, Rh(2), -(5), -(8), and -(9) and Rh(3), -(4), -(6), and -(12), is connected to four other rhodium atoms, two of which are coplanar with it, while the remaining two are located on the adjacent "internal" square. Each of the rhodium atoms Rh(10), -(11), -(15), and -(16) and Rh(1), -(7), -(13), and -(14) occupying one of the vertices of the "internal" squares is coordinated to five other rhodium atoms. A comparison of the diverse rhodium–rhodium distances (Table III) shows that an average length of 2.88 Å is found for the skeletal metal–metal bonding interactions on the surface, while shorter lengths are observed for the bonds involving the central rhodium atom, 2.76 Å. Moreover, it could be noted that intraplanar rhodium–rhodium distances of ~3.4 Å result in the absence of bonding interactions between the coplanar rhodium atoms placed on the "internal" squares.

The central rhodium atom is coordinated to the eight rhodium atoms located on the two internal squares. It is also bonded to the two sulfur atoms, S(1) and S(2), forming an encapsulated S–Rh–S moiety which is almost perfectly linear, 176.5°, with relatively short rhodium–sulfur bonds of 2.16 Å. In any case, the two sulfur–rhodium bonding lengths above are shorter than the sum of the covalent radii of rhodium, 1.38 Å, and of sulfur, 1.04 Å. This contraction of the metal–sulfur distance over those expected from the covalent radii of the elements involved has been also observed with other organometallic–chalcogen clusters.[23–33] The position of the sulfur atoms inside the cavities in between the external and internal planes results in bonding interactions between the sulfur atoms and the "basal" rhodium atoms of 2.33 Å. The longer edge for the internal rhodium planes (3.4 vs. 2.88 Å for the basal planes) may be the cause, or less likely the consequence, for

Table II. Final Positional Parameters, with Esd's, for $[C_6H_5N(C_2H_5)_3]_3[Rh_{17}(S)_2(CO)_{32}]^a$

atom	n	y	z	atom	n	y	z
				Anion			
Rh(1)	0.2472 (1)	0.09501 (4)	0.8604 (1)	C(12)	0.166 (2)	0.1775 (6)	0.477 (1)
Rh(2)	0.3177 (1)	0.21066 (4)	0.6018 (1)	O(12)	0.132 (1)	0.1942 (5)	0.477 (12)
Rh(3)	0.4250 (1)	0.03998 (4)	0.6791 (1)	C(13)	0.050 (2)	0.0602 (7)	0.587 (2)
Rh(4)	0.1806 (1)	0.03515 (5)	0.7545 (1)	O(13)	−0.009 (1)	0.0426 (5)	0.5508 (11)
Rh(5)	0.4123 (1)	0.21177 (4)	0.7746 (1)	C(14)	0.548 (2)	0.0685 (7)	0.839 (2)
Rh(6)	0.2378 (1)	0.03585 (4)	0.5942 (1)	O(14)	0.613 (1)	0.0525 (5)	0.8670 (12)
Rh(7)	0.3415 (1)	0.09723 (4)	0.5733 (1)	C(15)	0.526 (1)	0.1858 (6)	0.653 (1)
Rh(8)	0.1460 (1)	0.20639 (4)	0.6536 (1)	O(15)	0.582 (1)	0.2050 (4)	0.6384 (10)
Rh(9)	0.2410 (1)	0.20724 (5)	0.8291 (1)	C(16)	0.407 (2)	0.1827 (6)	0.955 (1)
Rh(10)	0.1346 (1)	0.14702 (4)	0.7662 (1)	O(16)	0.437 (1)	0.1974 (5)	1.0194 (11)
Rh(11)	0.3673 (1)	0.03930 (5)	0.8387 (1)	C(17)	0.083 (1)	0.1285 (6)	0.554 (1)
Rh(12)	0.2029 (1)	0.14928 (4)	0.5636 (1)	O(17)	0.007 (1)	0.1341 (4)	0.5122 (10)
Rh(13)	0.1285 (1)	0.09262 (4)	0.6432 (1)	C(18)	0.239 (1)	0.1125 (5)	0.484 (1)
Rh(14)	0.4626 (1)	0.09921 (4)	0.7874 (1)	O(18)	0.208 (1)	0.1055 (4)	0.4156 (9)
Rh(15)	0.4377 (1)	0.15391 (4)	0.6653 (1)	C(19)	0.154 (1)	0.1289 (5)	0.884 (1)
Rh(16)	0.3752 (1)	0.15168 (4)	0.8681 (1)	O(19)	0.120 (1)	0.1342 (4)	0.9427 (10)
Rh(17)	0.2910 (1)	0.12325 (4)	0.7168 (1)	C(20)	0.346 (1)	0.1135 (6)	0.946 (1)
S(1)	0.2982 (3)	0.0670 (1)	0.7146 (3)	O(20)	0.384 (1)	0.1075 (4)	1.0166 (10)
S(2)	0.2829 (4)	0.1796 (1)	0.7156 (3)	C(21)	0.401 (1)	0.2437 (6)	0.677 (1)
C(1)	0.214 (2)	0.0645 (6)	0.934 (1)	O(21)	0.434 (1)	0.2708 (4)	0.6658 (10)
O(1)	0.180 (1)	0.0476 (4)	0.9809 (10)	C(22)	0.209 (1)	0.2412 (6)	0.593 (1)
C(2)	0.353 (2)	0.2247 (7)	0.501 (2)	O(22)	0.187 (1)	0.2704 (5)	0.5660 (11)
O(2)	0.377 (1)	0.2326 (5)	0.4447 (13)	C(23)	0.455 (1)	0.0072 (6)	0.781 (1)
C(3)	0.537 (2)	0.0308 (7)	0.648 (2)	C(24)	0.480 (1)	−0.0193 (4)	0.7959 (10)
O(3)	0.605 (1)	0.0277 (5)	0.6287 (11)	O(24)	0.350 (1)	0.0053 (6)	0.603 (1)
C(4)	0.072 (2)	0.0230 (7)	0.786 (2)	O(24)	0.365 (1)	−0.0255 (4)	0.5761 (10)
O(4)	0.007 (1)	0.0164 (5)	0.8067 (12)	C(25)	0.046 (1)	0.1090 (6)	0.717 (1)
C(5)	0.529 (1)	0.2256 (7)	0.826 (2)	O(25)	−0.027 (1)	0.1010 (4)	0.7264 (10)
O(5)	0.604 (1)	0.2293 (5)	0.8610 (13)	C(26)	0.266 (2)	0.0044 (6)	0.837 (1)
C(6)	0.185 (1)	0.0226 (6)	0.485 (1)	O(26)	0.257 (1)	−0.0215 (4)	0.8735 (9)
O(6)	0.153 (1)	0.0172 (5)	0.4162 (11)	C(27)	0.170 (1)	0.0021 (6)	0.656 (1)
C(7)	0.383 (2)	0.0689 (6)	0.499 (1)	O(27)	0.142 (1)	−0.0268 (4)	0.6420 (9)
O(7)	0.419 (1)	0.0535 (5)	0.4510 (11)	C(28)	0.343 (1)	0.2434 (6)	0.840 (1)
C(8)	0.028 (2)	0.2156 (6)	0.603 (1)	O(28)	0.355 (1)	0.2715 (4)	0.8707 (10)
O(8)	−0.046 (1)	0.2223 (5)	0.5739 (11)	C(29)	0.501 (1)	0.1347 (5)	0.879 (1)
C(9)	0.210 (2)	0.2161 (7)	0.929 (2)	O(29)	0.574 (1)	0.1417 (4)	0.9199 (10)
O(9)	0.180 (1)	0.2187 (5)	0.9909 (12)	C(30)	0.534 (1)	0.1200 (6)	0.709 (1)
C(10)	0.044 (2)	0.1746 (7)	0.781 (2)	O(30)	0.610 (1)	0.1137 (5)	0.6947 (11)
O(10)	−0.024 (1)	0.1888 (4)	0.7946 (10)	C(31)	0.419 (1)	0.1366 (5)	0.549 (1)
C(11)	0.420 (2)	0.0315 (7)	0.950 (2)	O(31)	0.451 (1)	0.1438 (4)	0.4884 (10)
O(11)	0.450 (2)	0.0299 (6)	1.0218 (15)	C(32)	0.144 (1)	0.2381 (5)	0.757 (1)
				Cation			
N(1)	0.359 (1)	0.3933 (4)	0.4930 (9)	C(51)	0.145 (2)	0.4072 (7)	0.710 (2)
N(2)	0.240 (1)	0.3621 (5)	0.9785 (11)	C(52)	0.200 (2)	0.4026 (6)	0.790 (2)
N(3)	0.292 (2)	0.1621 (9)	0.2143 (21)	C(53)	0.153 (1)	0.3400 (6)	0.967 (1)
C(33)	0.313 (1)	0.3945 (6)	0.570 (1)	C(54)	0.167 (2)	0.3017 (6)	0.959 (2)
C(34)	0.377 (1)	0.3868 (5)	0.656 (1)	C(55)	0.311 (1)	0.3458 (6)	1.047 (1)
C(35)	0.409 (2)	0.4158 (7)	0.703 (2)	C(56)	0.285 (2)	0.3451 (6)	1.138 (2)
C(36)	0.465 (2)	0.4074 (7)	0.782 (2)	C(57)	0.213 (2)	0.3989 (6)	1.001 (1)
C(37)	0.483 (2)	0.3744 (7)	0.810 (2)	C(58)	0.293 (2)	0.4242 (7)	1.023 (2)
C(38)	0.450 (2)	0.3475 (7)	0.763 (2)	C(59)	0.281 (3)	0.1326 (2)	0.149 (3)
C(39)	0.392 (2)	0.3525 (7)	0.681 (1)	C(60)	0.262 (3)	0.0987 (11)	0.188 (3)
C(40)	0.394 (2)	0.3564 (7)	0.483 (2)	C(61)	0.165 (3)	0.0904 (11)	0.179 (3)
C(41)	0.319 (2)	0.3297 (10)	0.458 (2)	C(62)	0.149 (3)	0.0567 (12)	0.206 (3)
C(42)	0.280 (2)	0.4042 (7)	0.419 (2)	C(63)	0.211 (3)	0.0249 (13)	0.222 (3)
C(43)	0.318 (2)	0.4049 (8)	0.333 (2)	C(64)	0.296 (2)	0.0375 (10)	0.211 (2)
C(44)	0.443 (2)	0.4180 (7)	0.506 (2)	C(65)	0.319 (3)	0.0690 (12)	0.192 (3)
C(45)	0.420 (2)	0.4562 (8)	0.508 (2)	C(66)	0.351 (4)	0.1390 (15)	0.297 (3)
C(46)	0.283 (2)	0.3636 (6)	0.898 (1)	C(67)	0.451 (5)	0.1216 (18)	0.291 (4)
C(47)	0.217 (1)	0.3689 (6)	0.816 (1)	C(68)	0.206 (3)	0.1688 (11)	0.247 (2)
C(48)	0.191 (2)	0.3409 (7)	0.764 (1)	C(69)	0.133 (3)	0.1711 (10)	0.165 (2)
C(49)	0.137 (2)	0.3474 (7)	0.685 (2)	C(70)	0.347 (3)	0.1884 (12)	0.1901 (3)
C(50)	0.110 (2)	0.3812 (7)	0.655 (2)	C(71)	0.338 (3)	0.2243 (14)	0.233 (3)

^{a} Esd's, shown in parentheses, are right-adjusted to the least significant digits of the preceding numbers. They are derived from the inverse of the final least-squares matrix.

the absence of bonding interactions between the sulfur atoms and the rhodium atoms on the internal planes. Representative angles for $[Rh_{17}(S)_2(CO)_{32}]^{3-}$ are given in Table IV.

The coordination modes of the 32 carbonyl ligands are shown in Figure 2. Sixteen carbonyls are terminally bonded to an equal number of rhodium atoms, and the remaining carbonyls form reasonably symmetrical bridges. The eight bridging ligands on the basal planes are located along the edges, while the other bridging ligands are found along the rhodium–rhodium bonds connecting the two internal planes.

General Structural Considerations. The rhodium–rhodium distances present in $[Rh_{17}(S)_2(CO)_{32}]^{3-}$ are similar to those found in other clusters (e.g., $Rh_4(CO)_{12}$, 2.73;[1] $Rh_6(CO)_{16}$, 2.78;[1] $Rh_8(CO)_{19}C$, 2.81;[35] $[Rh_{12}(CO)_{30}]^{2-}$, 2.79; [Rh₁₅-

Table III. Interatomic Distances (A) and Estimated Esd's for $[C_6H_5CH_2N(C_2H_5)_3]_3[Rh_{17}(S)_2(CO)_{32}]$

$[Rh_{17}(S)_2(CO)_{32}]^{3-}$

(a) Distances for Rhodium–Rhodium Bonds

Intra Basal Planes

Rh(2)-Rh(5)	2.882 (2)	Rh(4)-Rh(6)	2.890 (2)
Rh(2)-Rh(8)	2.885 (2)	Rh(4)-Rh(12)	2.868 (2)
Rh(3)-Rh(6)	2.879 (2)	Rh(5)-Rh(9)	2.880 (2)
Rh(3)-Rh(12)	2.885 (2)	Rh(8)-Rh(9)	2.882 (2)

Inter Basal–Internal Planes

Rh(1)-Rh(4)	2.929 (2)	Rh(5)-Rh(16)	2.877 (2)
Rh(1)-Rh(12)	2.863 (2)	Rh(6)-Rh(7)	2.833 (2)
Rh(2)-Rh(11)	2.976 (2)	Rh(6)-Rh(13)	2.931 (2)
Rh(2)-Rh(15)	2.887 (2)	Rh(8)-Rh(10)	2.920 (2)
Rh(3)-Rh(7)	2.918 (2)	Rh(8)-Rh(11)	2.883 (2)
Rh(3)-Rh(14)	2.864 (2)	Rh(9)-Rh(10)	2.882 (2)
Rh(4)-Rh(13)	2.863 (2)	Rh(9)-Rh(16)	2.918 (2)
Rh(5)-Rh(15)	2.915 (2)	Rh(12)-Rh(14)	2.916 (2)

Inter Internal Planes

Rh(1)-Rh(10)	2.860 (2)	Rh(10)-Rh(13)	2.879 (2)
Rh(1)-Rh(16)	2.890 (2)	Rh(11)-Rh(13)	2.867 (2)
Rh(7)-Rh(11)	2.867 (2)	Rh(14)-Rh(15)	2.863 (2)
Rh(7)-Rh(15)	2.866 (2)	Rh(14)-Rh(16)	2.858 (2)

Central–Surface Rhodium

Rh(1)-Rh(17)	2.761 (2)	Rh(13)-Rh(17)	2.758 (2)
Rh(7)-Rh(17)	2.770 (2)	Rh(14)-Rh(17)	2.763 (2)
Rh(10)-Rh(17)	2.774 (2)	Rh(15)-Rh(17)	2.756 (2)
Rh(11)-Rh(17)	2.763 (2)	Rh(16)-Rh(17)	2.756 (2)

(b) Rhodium–Sulfur Lengths

Sulfur–Basal Rhodium

Rh(2)-S(2)	2.334 (4)	Rh(3)-S(1)	2.336 (4)
Rh(4)-S(2)	2.330 (5)	Rh(4)-S(1)	2.339 (4)
Rh(8)-S(2)	2.341 (5)	Rh(6)-S(1)	2.319 (4)
Rh(9)-S(2)	2.321 (51)	Rh(12)-S(1)	2.332 (4)

Sulfur–Internal Rhodium

Rh(1)-S(1)	2.834 (2)	Rh(10)-S(2)	2.882 (5)
Rh(7)-S(1)	2.759 (4)	Rh(11)-S(2)	2.781 (5)
Rh(13)-S(1)	2.762 (4)	Rh(15)-S(2)	2.773 (5)
Rh(14)-S(1)	2.804 (4)	Rh(16)-S(2)	2.796 (5)

Sulfur–Central Rhodium

Rh(17)-S(1)	2.166 (4)	Rh(17)-S(2)	2.170 (4)

(c) Rhodium–Carbonyl Bond Lengths

Basal Terminal

Rh(2)-C(2)	1.88 (2)	Rh(6)-C(6)	1.86 (2)
Rh(3)-C(3)	1.88 (2)	Rh(8)-C(8)	1.84 (2)
Rh(4)-C(4)	1.86 (3)	Rh(9)-C(9)	1.80 (3)
Rh(5)-C(5)	1.87 (2)	Rh(12)-C(12)	1.84 (3)

Intra Basal Plane Bridge

Rh(2)-C(21)	2.02 (2)	Rh(6)-C(24)	2.04 (2)
Rh(2)-C(22)	1.99 (2)	Rh(6)-C(27)	2.02 (2)
Rh(3)-C(23)	2.05 (2)	Rh(8)-C(22)	2.03 (2)
Rh(3)-C(24)	2.01 (2)	Rh(8)-C(32)	2.05 (2)
Rh(4)-C(26)	2.05 (2)	Rh(9)-C(28)	2.05 (2)
Rh(4)-C(27)	2.03 (2)	Rh(9)-C(32)	2.05 (2)
Rh(5)-C(21)	1.99 (2)	Rh(12)-C(23)	2.05 (2)
Rh(5)-C(28)	2.03 (2)	Rh(12)-C(26)	2.02 (3)

(c) Rhodium–Carbonyl Bond Lengths (*Continued*)

Internal Terminal

Rh(1)-C(1)	1.81 (2)	Rh(13)-C(13)	1.83 (2)
Rh(7)-C(7)	1.82 (2)	Rh(14)-C(14)	1.82 (2)
Rh(10)-C(10)	1.78 (2)	Rh(15)-C(15)	1.84 (2)
Rh(11)-C(11)	1.77 (2)	Rh(16)-C(16)	1.83 (2)

Inter Internal Plane Bridge

Rh(1)-C(19)	2.01 (2)	Rh(13)-C(17)	2.01 (2)
Rh(1)-C(20)	1.95 (3)	Rh(13)-C(25)	1.90 (2)
Rh(7)-C(18)	1.99 (2)	Rh(14)-C(24)	2.02 (2)
Rh(7)-C(31)	2.00 (2)	Rh(14)-C(30)	1.98 (2)
Rh(10)-C(19)	2.00 (2)	Rh(15)-C(30)	1.97 (2)
Rh(10)-C(25)	2.03 (2)	Rh(15)-C(31)	1.96 (2)
Rh(11)-C(17)	1.95 (2)	Rh(16)-C(20)	2.03 (2)
Rh(11)-C(18)	2.05 (2)	Rh(16)-C(29)	1.97 (2)

(d) Carbonyl C–O Lengths

Basal Terminal

C(2)-O(2)	1.10 (2)	C(6)-O(6)	1.15 (2)
C(3)-O(3)	1.13 (2)	C(8)-O(8)	1.15 (2)
C(4)-O(4)	1.12 (2)	C(9)-O(9)	1.18 (2)
C(5)-O(5)	1.15 (2)	C(12)-O(12)	1.17 (2)

Intra Basal Plane Bridge

C(21)-O(21)	1.18 (2)	C(26)-O(26)	1.17 (2)
C(22)-O(22)	1.23 (2)	C(27)-O(27)	1.19 (2)
C(23)-O(23)	1.15 (2)	C(28)-O(28)	1.19 (2)
C(24)-O(24)	1.19 (2)	C(32)-O(32)	1.14 (2)

Internal Terminal

C(1)-O(1)	1.18 (2)	C(13)-O(13)	1.18 (2)
C(7)-O(7)	1.19 (2)	C(14)-O(14)	1.16 (2)
C(10)-O(10)	1.21 (2)	C(15)-O(15)	1.17 (2)
C(12)-O(12)	1.20 (2)	C(16)-O(16)	1.20 (2)

Inter Internal Planes Bridge

C(17)-O(17)	1.22 (2)	C(25)-O(25)	1.18 (2)
C(18)-O(18)	1.14 (2)	C(29)-O(29)	1.20 (2)
C(19)-O(19)	1.18 (3)	C(30)-O(30)	1.23 (2)
C(20)-O(20)	1.20 (2)	C(31)-O(31)	1.21 (2)

$[C_6H_5CH_2N(C_2H_5)_3]^+$

(e) Carbon–Carbon and Carbon–Nitrogen Distances

N(1)-C(33)	1.54 (2)	C(44)-C(45)	1.51 (3)
N(1)-C(40)	1.54 (2)	C(46)-C(47)	1.52 (2)
N(1)-C(42)	1.57 (2)	C(47)-C(48)	1.37 (2)
N(1)-C(44)	1.57 (2)	C(47)-C(52)	1.37 (2)
N(2)-C(46)	1.56 (2)	C(48)-C(49)	1.40 (3)
N(2)-C(53)	1.54 (2)	C(49)-C(50)	1.47 (3)
N(2)-C(55)	1.52 (2)	C(50)-C(51)	1.38 (3)
N(2)-C(57)	1.54 (2)	C(51)-C(52)	1.41 (3)
N(3)-C(59)	1.53 (4)	C(53)-C(54)	1.50 (2)
N(3)-C(66)	1.69 (4)	C(55)-C(56)	1.59 (3)
N(3)-C(68)	1.51 (4)	C(57)-C(58)	1.53 (3)
N(3)-C(70)	1.41 (4)	C(59)-C(60)	1.51 (4)
C(33)-C(34)	1.55 (2)	C(60)-C(61)	1.46 (4)
C(34)-C(35)	1.39 (3)	C(60)-C(65)	1.42 (5)
C(34)-C(39)	1.38 (2)	C(61)-C(62)	1.42 (5)
C(35)-C(36)	1.43 (3)	C(62)-C(63)	1.53 (5)
C(36)-C(37)	1.36 (3)	C(63)-C(64)	1.39 (5)
C(37)-C(38)	1.31 (3)	C(64)-C(65)	1.31 (5)
C(38)-C(39)	1.45 (3)	C(66)-C(67)	1.66 (6)
C(39)-C(40)	1.34 (3)	C(68)-C(69)	1.60 (4)
C(40)-C(41)	1.51 (3)	C(70)-C(71)	1.55 (5)
C(42)-C(43)	1.60 (3)		

$C_2(CO)_{28}]^-$, 2.87;[37] and $[Rh_{13}(CO)_{24}H_3]^{2-}$, 2.81 Å[17]), although a simple comparison with these and other clusters[1] indicates that the average value of 2.88 Å observed for the surface rhodium–rhodium bonding distance is among the longest reported for this kind of compound. A similar trend in the lengths of the rhodium–rhodium bonds has been previously suggested to introduce a certain degree of destabilization in $[Rh_{15}(CO)_{28}C_2]^-$, but it is evident from the unusual stability of $[Rh_{17}(S)_2(CO)_{32}]^{3-}$ (vide infra) that the argument is not

applicable to the latter anion. It is obvious that the rhodium–rhodium bonds involving the central rhodium atom of $[Rh_{17}(S)_2(CO)_{32}]^{3-}$ are significantly shorter than those on the surface. A comparison of the surface vs. internal distances in clusters containing central rhodium atoms such as $[Rh_{13}(CO)_{24}H_3]^{2-}$[17] and $[Rh_{15}(C)_2(CO)_{28}]^{-}$[37] shows that no significant differences are found between those distances. A 12-coordinate central metal atom of an icosahedron, like that present in $[Rh_{13}(CO)_{24}H_3]^{2-}$, should result in metal–metal

Table IV. Representative Angles with Esd's (deg) within $[Rh_{17}(S)_2(CO)_{32}]^{3-}$ [a]

(a) Angles of the Rhodium Framework

Rh(5)-Rh(2)-Rh(8)	90.11 (6)	Rh(2)-Rh(11)-Rh(7)	99.34 (6)
Rh(6)-Rh(4)-Rh(11)	89.69 (6)	Rh(11)-Rh(7)-Rh(15)	98.28 (5)
Rh(2)-Rh(11)-Rh(8)	59.68 (5)	Rh(7)-Rh(15)-Rh(2)	99.41 (6)
Rh(4)-Rh(1)-Rh(11)	59.36 (5)	Rh(10)-Rh(17)-Rh(11)	81.82 (5)
Rh(9)-Rh(5)-Rh(16)	50.91 (5)	Rh(11)-Rh(17)-Rh(15)	80.93 (5)
Rh(11)-Rh(2)-Rh(15)	76.38 (5)	Rh(7)-Rh(11)-Rh(17)	58.92 (5)

(b) Angles of the Rhodium-Sulfur Framework

Rh(2)-S(2)-Rh(5)	76.3 (1)	S(2)-Rh(17)-Rh(10)	68.4 (1)
Rh(5)-S(2)-Rh(8)	121.8 (2)	S(2)-Rh(17)-Rh(7)	111.9 (1)
Rh(2)-S(2)-Rh(17)	120.0 (2)	S(2)-Rh(17)-Rh(14)	112.2 (1)
S(1)-Rh(17)-S(2)	178.5 (2)	S(1)-Rh(17)-Rh(10)	112.4 (1)

(c) Angles Involving Carbonyl Groups

Rh(8)-C(8)-O(8)	176 (2)	Rh(2)-C(22)-O(22)	132 (1)
Rh(11)-C(11)-O(11)	173 (2)	C(30)-Rh(15)-C(31)	94.4 (7)
Rh(5)-C(5)-O(5)	170 (2)	C(31)-Rh(7)-C(7)	92.1 (8)
Rh(2)-C(2)-O(2)	177 (2)	C(6)-Rh(6)-C(27)	97.5 (8)
Rh(2)-C(22)-Rh(8)	91.8 (8)	C(24)-Rh(6)-C(27)	95.0 (7)

[a] A complete list of the angles within $[Rh_{17}S_2(CO)_{32}]^{3-}$ and the $[C_6H_5CH_2N(C_2H_5)_3]^+$ cations is available as supplementary material.
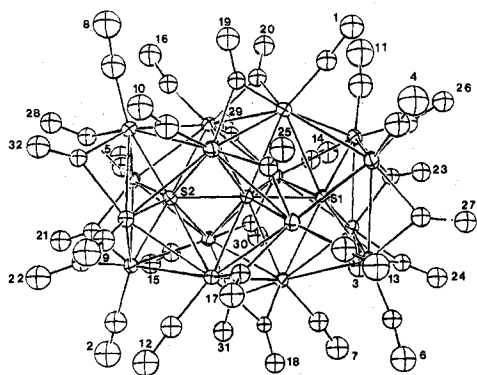
Figure 2. ORTEP diagram of $[Rh_{17}(S)_2(CO)_{32}]^{3-}$ showing also the carbon monoxide ligands.

contacts of equal lengths.[35] In contrast, 10-coordination around a central atom is expected if a typical body-centered cubic packed structure is compressed along the fourfold axis,[40] parallel in this case to the S–Rh–S bonds. Thus, an ideal structure with body-centered tetragonal packing should result.[40] Instead, the distortion from this ideal structure resulting in the sulfur bicapped cubic antiprismatic arrangement present around this central rhodium atom of $[Rh_{17}(S)_2(CO)_{32}]^{3-}$ could be partially ascribed to the steric requirements of the carbonyl ligands coordinated on this section of the cluster (vide infra).

The adoption of the distorted square prism distribution of rhodium atoms present in $[Rh_{17}(S)_2(CO)_{32}]^{2-}$ could be attributed more specifically to other additional factors. The encapsulation of atoms with a covalent radius larger than 1.0 Å by a rhodium–carbonyl cluster could be expected to result in a cubic arrangement of metal atoms, based exclusively on steric factors.[1] Then, the cubic antiprismatic structure of the anion is at least partially attributed to the steric demands of the encapsulated sulfur atoms as inferred from the significantly short sulfur–rhodium distances for the Rh(17)–S(1) and Rh(17)–S(2) bonds. The closeness of the two sulfur atoms to the central rhodium, together with the space requirements of these atoms, could be responsible for the expansion of the intraplanar rhodium–rhodium interatomic distance beyond that expected from normal bonding interactions. Moreover, repulsions between the carbonyl ligands should also be influencing the adoption of the structure with staggered rhodium planes instead of eclipsed ones. A similar situation may be found in $[Rh_6(CO)_{15}C]^{2-}$ where there appear to be repulsive interactions between the carbonyl ligands located on the parallel planes whose interplanar separation is similar to that

Table V. Comparison of Carbonyl Distribution in Some Examples of High-Nuclearity Rhodium-Carbonyl Clusters

	$[Rh_{13}-(CO)_{24}-H_3]^{2-}$	$[Rh_{15}-(C)_2-(CO)_{28}]^-$	$[Rh_{17}-(S)_2-(CO)_{32}]^{3-}$
surface Rh atoms	12	14	16
CO:Rh total	1.85	1.87	1.85
CO:Rh surface	2.0	2.0	2.0
range of C--C, Å	2.5–3.3	2.6–3.3	2.6–3.4

of the sulfido anion.[41] In addition, while both potential conformations of $[Rh_{17}(S)_2(CO)_{32}]^{3-}$ have the same number of rhodium–carbon bonds, the eclipsed structure results in the formation of four additional rhodium–rhodium bonds.

Indications of carbonyl crowding are present even in the structure of a cluster as large as $[Rh_{17}(S)_2(CO)_{32}]^{3-}$ as concluded from the carbon–carbon distances. Interligand carbon–carbon contacts are in the range of 2.5–3.6 Å (basal planes: 2.52 Å, terminal–bridge; 2.90 Å, bridge–bridge; internal planes: 2.52 Å, terminal–bridge; 3.12 Å, bridge–bridge; 3.25 Å, terminal internal–bridge basal; 3.60 Å, bridge internal–terminal basal and terminal internal–terminal basal) and they indicate that ligand overcrowding is similar to that found in other rhodium–carbonyl clusters.[1-3] A comparison of the range of carbon–carbon distances for three high-nuclearity rhodium–carbonyl clusters (Table V) suggests that the curvature of the surface of the metal polyhedron is more important than its size in determining the sector of space per cluster atom that remains available for the ligands.

The rhodium–carbonyl interactions result in rhodium–carbon distances (Table III) for the terminal and bridging carbonyls coordinated to the basal rhodium atoms of 1.85 and 2.03 Å, respectively, and values of 1.81 and 1.99 Å for similar distances for the rhodium atoms placed in the internal planes. The C–O distances for terminal and bridging carbonyls bonded to basal and to internal rhodium atoms are 1.14 and 1.18 and 1.18 and 1.20 Å, respectively. These values are similar to those reported for other rhodium–carbonyl clusters.[1,2] The differences in the C–O distance for the terminal ligands coordinated to the rhodium in the internal and basal planes of $[Rh_{17}(S)_2(CO)_{32}]^{3-}$ should result from differences in the metal–carbonyl interactions giving lower metal to ligand back-bonding for the basal planes ligands (basal ligands: Rh–C = 1.85 Å, C–O = 1.14 Å; internal planes ligands: Rh–C = 1.81 Å, C–O = 1.18 Å). The lesser extent of back-bonding for these ligands is perhaps a consequence of the electron-withdrawing effect of the sulfide atoms coordinated to the basal rhodium atoms.
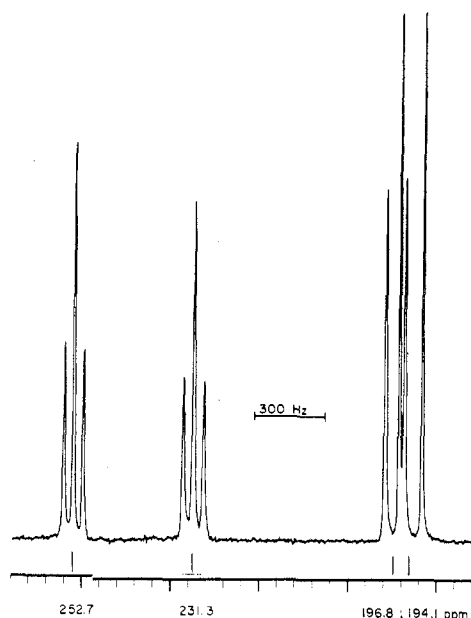
Figure 3. ^{13}C NMR spectrum of $[Rh_{17}(S)_2(CO)_{32}]^{3-}$ at 40 °C. Chemical shifts of carbon resonance bands for the carbonyl ligands are given in ppm downfield from tetramethylsilane.

The bond angles for the Rh–C–O moieties indicate linear interactions for the terminal carbonyls with mean values of 174.3 and 171.2° for the basal and internal ligands. The bridging groups for the basal planes are reasonably symmetrical, and they exhibit Rh–C–O and Rh–C–Rh angles of 134.6 and 90.7°. The bridge carbonyls coordinated on the internal planes are moderately asymmetric, with Rh–C–O and Rh–C–Rh angular values of 134.3 and 92.1°.

Nuclear Magnetic Resonance Studies. The proton NMR of an acetone-d_6 solution (0.8 g in 2.0 mL) of $[C_6H_5CH_2-N(C_2H_5)_3]_3[Rh_{17}(S)_2(CO)_{32}]$ was studied looking for any resonance bands indicative of either metallic hydrides or carbon- and sulfur-bonded hydrogen atoms. The only bands detected are those expected for the cation. There are no observable resonance bands corresponding to metallic hydrides even after Fourier scanning of the solution for 12 h up to 50 ppm upfield from tetramethylsilane.

^{13}C NMR of the solution (Figure 3) resulted in two sets of triplets with chemical shifts of 252.7 and 231.3 ppm and coupling constants of 40.9 and 44.5 Hz, respectively, which are assigned to bridge carbonyls (rhodium spin number $^1/_2$), while the two sets of doublets with chemical shifts of 196.8 and 194.1 ppm and coupling constants of 83.9 and 97.3 Hz are assigned to terminally bonded carbonyl ligands. These values for the chemical shifts and coupling constants for terminal bridge bonded carbonyls are similar to those recently reported for related compounds.[1,43-46]

The presence of two different types of terminal and bridging carbonyl resonances in an intensity ratio of 1:1:1:1 is in agreement with the presence of four equivalent groups of eight carbonyls ligands each, in the solid structure of $[Rh_{17}(S)_2(CO)_{32}]^{3-}$. Moreover, the relative height of these multiplets appears to indicate fluxionality for the upfield triplet and the lower field doublet. In general, it has been noted that an increase in rhodium–carbon bond distances results in a decrease in the rhodium–carbon coupling constant of the Rh–CO bonds and in lower chemical shifts.[1,42-45] These arguments allow the assignments of the ^{13}C resonances corresponding to the bridge carbonyls (Table VI) to be applied with a certain degree of confidence, but a more ambiguous situation is found for the two resonances corresponding to the terminal ligands, as a result of their similar chemical shifts. It is expected that

Table VI. ^{13}C NMR Results[a] and Suggested Assignments for $[Rh_{17}(S)_2(CO)_{32}]^{3-}$

chem shifts, ppm	252.7, 231.8	195.8, 194.1
J(Rh–CO), Hz	40.9, 44.5	83.9, 97.3
assign	Rh–CO–Rh	Rh–CO
probable location on Rh planes	basal, internal	
$\bar{d}$(Rh–CO), Å	2.03, 1.99	1.85, 1.81

[a] Spectra recorded at probe temperatures of 40 °C.
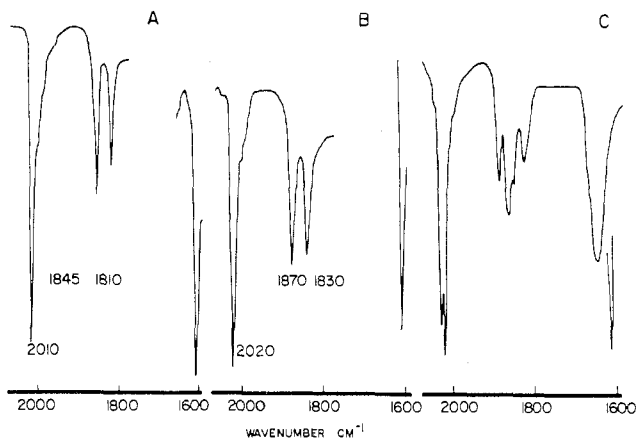
Figure 4. Infrared spectra: (A) $[Rh_{17}(S)_2(CO)_{32}]^{3-}$, (B) $[Rh_{17}-(S)_2(CO)_{32}H_n]^{(3-n)-}$, (C) a mixture of the two previous spectra obtained upon acidification of (A) with less than stoichiometric amounts of acid. All spectra were taken in acetone solutions.

variable-temperature ^{13}C NMR studies actually underway on the latter would help in completing the present assignments.

Derivatives and Reactivity. The $[Cs(18-crown-6)_{2-3}]^+$, K^+, and NH_4^+ salts of the anion have been easily obtained either by using the corresponding carboxylic acid salts in place of cesium benzoate in the synthetic procedure or by the corresponding metathesis reactions. These compounds, as well as the benzyltriethylammonium salt, are soluble in acetone, acetonitrile, tetrahydrofuran, and dimethyl sulfoxide but insoluble in water and nonpolar organic solvents. These salts are stable to air and moisture.

In contrast to the facile reactivity of rhodium–carbonyl clusters in the presence of bases,[1,3] $[Rh_{17}(S)_2(CO)_{32}]^{3-}$ has been found to be stable under an atmosphere of carbon monoxide in the presence of highly basic media in aqueous glyme (400:1 KOH:cluster molar ratio) or tetrahydrofuran (100:1 CsOH:cluster molar ratio) as indicated by the persistence of the infrared spectrum of the anion (Figure 4) after 300 h of contact time.

Similar resistance to demolition is exhibited by the anionic cluster under moderately acidic conditions, although reaction does occur as indicated by the high-frequency shifts of the bands present in the infrared spectrum of the initial cluster (Figure 4). This shift is indicative of a reduction in the extent of back-bonding from the cluster's molecular orbitals to the carbonyl ligands. Our ability to regenerate the initial spectrum on addition of base to the resulting solution, working in the absence of carbon monoxide, is indicative of the protonation of the anion. In addition, the solid isolated from the acidified solution has elemental Cs:Rh:S ratios of 1:17:2 which suggests that diprotonation of the initial anion may have been achieved.

The ability of $[Rh_{17}(S)_2(CO)_{32}]^{3-}$ to exhibit similar Brønsted acid–base chemistry as that previously reported for $[Rh_{13}(CO)_{24}H_3]^{2-}$[12] has been demonstrated by infrared monitoring of successive acid and base treatments (eq 3, Figure

$$[Rh_{17}(S)_2(CO)_{32}]^{3-} \underset{OH^-}{\overset{H^+}{\rightleftharpoons}} \text{``}[Rh_{17}(S)_2H_2(CO)_{32}]^-\text{''} \qquad (3)$$
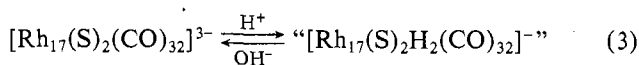
4). We have conducted several unsuccessful ^1H NMR ex-

periments aimed at detecting the presence of the protons in the final material isolated after acid treatment of $[Rh_{17}(S)_2(CO)_{32}]^{3-}$. At this point, the absence of any detectable proton resonance has precluded us from confirming the presence of proton in this product or to propose a coordination mode for them.

We have also evaluated the ability of $[Rh_{17}(S)_2(CO)_{32}]^{3-}$ to activate molecular hydrogen at 25 °C and 1 atm by reacting the cesium salt of the cluster with phenyl glyoxal and hydrogen in tetrahydrofuran. Isolation of the main component of the mixture ($\sim 30\%$), after a reaction time of about 48 h, resulted in the identification of $C_6H_5CHOHCH_3$, as concluded from proton NMR and mass spectral analysis of the material. The homogeneity of the final solution and the persistence of the infrared pattern of the initial anion (together with some spectral indications for the presence of minor amounts of $[Rh_{17}(S)_2(CO)_{32}H_n]^{(3-n)-}$) suggest that the initial anion may be able to catalytically activate molecular hydrogen under our conditions.

Final Observations

The characterization of $[Rh_{17}(S)_2(CO)_{32}]^{3-}$ has shown that the known ability of transition-metal–carbonyl clusters for the encapsulation of main-element atoms, which was previously limited to carbon, e.g., $[Rh_6(CO)_{15}C]^{2-}$, $[Rh_{15}(C)_2(CO)_{28}]^{-}$, ... , is a more general property which can be extended to other main-group elements, such as sulfur. Other relevant analogies between carbido and sulfido clusters are present in the cases of $[Rh_{15}(C)_2(CO)_{28}]^{-37}$ and $[Rh_{17}(S)_2(CO)_{32}]^{3-}$. Both anionic species provide examples of the encapsulation of the E–Rh–E group by transition-metal clusters (E = C and S).

The analogies suggest that the arguments applied in explaining the stability of $[Rh_{15}(C)_2(CO)_{28}]^{-}$ could be possibly extended to $[Rh_{17}(S)_2(CO)_{32}]^{3-}$. Steric effects, in specific interactions between ligands, seem to be determinant of the stability of large clusters, and it has been mentioned[37] that the presence of two carbido atoms in $[Rh_{15}(C)_2(CO)_{32}]^{3-}$ could be introducing additional stability in this cluster by the ability of the carbon atoms to donate four pairs of electrons without the volume demands of other type of ligands. The evidence accumulated by us indicates that the sulfur atoms present in the bis(sulfido) anion are sharing all of their outer-shell electrons, in a manner similar to that found in $[Fe_2(CO)_6(\mu\text{-}SCH_3)]_2S$.[32] The ability of these atoms to donate a total of six electron pairs to the cluster, without steric hindrance and without providing additional negative charge, may be then an important reason in the unusual stability of the cluster. Additional reasons for the stability of $[Rh_{17}(S)_2(CO)_{32}]^{3-}$ could be attributed in a more simplistic fashion to the presence of one encapsulated sulfur atom in each of the cluster sections and to the ability of these atoms to "glue together" the diverse sections of the cluster as suggested by the mode of coordination of these atoms and as expected from the high rhodium–sulfur bond affinity.[46] Finally, the high stability and the low carbonyl:metal ratio of this cluster are in agreement with previous predictions[1] indicating that stable high-nuclearity clusters would require low carbonyl:metal ratios.

The arrangement of rhodium atoms found in $[Rh_{17}(S)_2(CO)_{32}]^{3-}$ is an example of body-centered cubic packing of metal atoms, or, more precisely, it is an example of tetragonal distortion of that arrangement.[40] This report constitutes the first instance in which such an arrangement is found in a rhodium cluster. The occurrence of this structure in a rhodium–carbonyl cluster expands the number of metal polyhedra known to be formed by these clusters and it offers one more instance of the previously noted versatility of rhodium in giving a large variety of clusters.[37]

Two other comments can be added. First, it is evident from the chemical properties of $[Rh_{17}(S)_2(CO)_{32}]^{3-}$ and $[Rh_6(CO)_{15}C]^{2-41}$ that clusters of similar stability could perhaps be prepared by encapsulation of other main-element atoms, e.g., P.[47] Second, the formation of this cluster could be indicative of the need for drastic experimental conditions in the preparation of high-nuclearity clusters with cubic packing of metal atoms. The thermodynamic balance of the rhodium–rhodium vs. rhodium–carbonyl bonds[1] indicates that conditions of increased temperature, and possibily of increased temperature and pressure of carbon monoxide, are favorable for the formation of high-nuclearity clusters.

Further reports will illustrate results along these lines as well as other aspects of the reactivity and behavior of $[Rh_{17}(S)_2(CO)_{32}]^{3-}$.[48]

Registry No. $Rh(CO)_2acac$, 14874-82-9; $[C_6H_5CH_2N(CH_2C-H_3)_3]_3[Rh_{17}(S)_2(CO)_{32}]$, 67382-20-1; $[Cs(C_{12}H_{24}O_6)_2]_3[Rh_{17}(S)_2(CO)_{32}]$, 67382-19-8; $[Rh_{17}(S)_2(CO)_{32}]CsH_2$, 67350-76-9.

Supplementary Material Available: A table of observed and calculated structure factors, a table of root-mean-square amplitudes of thermal vibration, complete tables for the bond distances and angles for the anion and the cation, as well as tables for the positional and thermal parameters and for the general temperature factor expressions (42 pages). Ordering information is given on any current masthead page.

References and Notes

(1) P. Chini, G. Longoni, and V. G. Albano, *Adv. Organomet. Chem.*, **14**, 285 (1976).
(2) J. Lewis and B. F. G. Johnson, *Pure Appl. Chem.*, **44**, 43 (1975).
(3) P. Chini, *Inorg. Chim. Acta*, **2**, 31 (1968).
(4) E. L. Muetterties, *Science*, **196**, 839 (1977).
(5) E. L. Muetterties, *Bull. Soc. Chim. Belg.*, **84**, 959 (1975).
(6) E. L. Muetterties, *Bull. Soc. Chim. Belg.*, **85**, 451 (1976).
(7) T. H. Whitesides and R. A. Budnik, *J. Chem. Soc., Chem. Commun.*, 87 (1973).
(8) A. J. Deeming and M. Underhill, *J. Organomet. Chem.*, **42**, C60 (1972).
(9) K. G. Caulton, M. G. Thomas, B. A. Sosinsky, and E. L. Muetterties, *Proc. Natl. Acad. Sci. U.S.A.*, **73**, 4274 (1976).
(10) G. C. Demitras and E. L. Muetterties, *J. Am. Chem. Soc.*, **99**, 2796 (1977).
(11) M. G. Thomas, B. F. Beier, and E. L. Muetterties, *J. Am. Chem. Soc.*, **98**, 1296 (1976).
(12) V. A. Albano, A. Ceriotti, P. Chini, G. Ciani, S. Martinengo, and W. M. Anker, *J. Chem. Soc., Chem. Commun.*, 859 (1975).
(13) R. L. Pruett and W. E. Walker, U.S. Patent 3,957,857.
(14) W. E. Walker and E. S. Brown, U.S. Patent 3,968,136; E. S. Brown et al., U.S. Patents 3,929,969, 3,878,292, and 3,878,290.
(15) R. L. Pruett and W. E. Walker, Formation of Ethylene Glycol from Synthesis Gas, Symposium on Organometallic Chemistry, Leeds, England, 1976.
(16) J. L. Vidal, R. A. Fiato, L. A. Cosby, and R. L. Pruett, and J. L. Vidal, W. E. Walker, D. R. Bryant, L. A. Cosby, and R. L. Pruett, Ninth Regional Meeting of the American Chemical Society, Charleston, W. Va., October 1977; J. L. Vidal, L. A. Cosby, R. A. Fiato, W. E. Walker, and R. L. Pruett, 174th National Meeting of the American Chemical Society, Anaheim, Calif., March 1978.
(17) S. Martinengo, B. T. Heaton, R. J. Goodfellow, and P. Chini, *J. Chem. Soc., Chem. Commun.*, 39 (1977).
(18) A. J. Deeming and M. Underhill, *J. Chem. Soc., Chem. Commun.*, 277 (1973).
(19) J. Evans, B. F. G. Johnson, J. Lewis, and T. W. Matheson, *J. Organomet. Chem.*, **97**, C16 (1975).
(20) E. H. Braye, L. F. Dahl, W. Hubel, and D. L. Wampler, *J. Am. Chem. Soc.*, **84**, 4633 (1962).
(21) V. Albano, M. Sansoni, P. Chini, and S. Martinengo, *J. Chem. Soc., Dalton Trans.*, 651 (1973).
(22) G. Schmid, V. Batzel, G. Etrzodt, and R. Pfeil, *J. Organomet. Chem.*, **86**, 257 (1975); **112**, 345 (1976).
(23) G. L. Simon and L. F. Dahl, *J. Am. Chem. Soc.*, **95**, 2175 (1973).
(24) A. S. Foust, M. S. Foster, and L. F. Dahl, *J. Am. Chem. Soc.*, **91**, 5631 (1969).
(25) L. F. Dahl and P. W. Sutton, *Inorg. Chem.*, **2**, 1067 (1963).
(26) G. L. Simon and L. F. Dahl, *J. Am. Chem. Soc.*, **95**, 2174 (1973).
(27) L. F. Dahl and C. H. Wei, *Inorg. Chem.*, **2**, 328 (1963).
(28) C. H. Wei, L. Marko, G. Bor, and L. F. Dahl, *J. Am. Chem. Soc.*, **95**, 4840 (1973).

(29) C. H. Wei and L. F. Dahl, *Cryst. Struct. Commun.*, **4**, 583 (1975).
(30) C. H. Wei and L. F. Dahl, *Inorg. Chem.*, **6**, 1229 (1967).
(31) D. L. Stevenson, H. C. Wei, and L. F. Dahl, *J. Am. Chem. Soc.*, **93**, 6027 (1971).
(32) J. M. Coleman, A. Wojcicki, P. J. Pollick, and L. F. Dahl, *Inorg. Chem.*, **6**, 1236 (1967).
(33) C. H. Wei and L. F. Dahl, *Inorg. Chem.*, **4**, 493 (1965).
(34) S. Martinengo, B. T. Heaton, R. J. Goodfellow, and P. Chini, *J. Chem. Soc., Chem. Commun.*, 39 (1977).
(35) V. Albano, P. Chini, S. Martinengo, and M. Sansoni, *J. Chem. Soc., Chem. Commun.*, 299 (1974).
(36) V. Albano, P. Chini, G. Ciani, S. Martinengo, and M. Sansoni, paper presented at the VIIth Congresso Nazionali Chimica Inorganica, Perma, 1974, and private communication.
(37) V. Albano, P. Chini, S. Martinengo, and M. Sansoni, *J. Chem. Soc., Chem. Commun.*, 299 (1974); *J. Chem. Soc., Dalton Trans.*, 305 (1975).
(38) D. T. Cromer and J. T. Waber, "International Tables for X-Ray Crystallography", Vol. IV, Kynoch Press, Birmingham, England, in preparation.
(39) D. T. Cromer and D. Lieberman, *J. Chem. Phys.*, **53**, 1891 (1970).
(40) A. F. Wells, "Structural Inorganic Chemistry", 3rd ed., Clarendon Press, London, 1962.
(41) V. Albano, M. Sansoni, P. Chini, and S. Martinengo, *J. Chem. Soc., Dalton Trans.*, 651 (1973).
(42) V. Albano, P. Bellon, and C. F. Ciani, *Chem. Commun.*, 1024 (1969).

(43) B. Heaton, A. Towl, P. Chini, A. Fumagalli, D. McCaffrey, and S. Martinengo, *J. Chem. Soc., Chem. Commun.*, 523 (1975).
(44) F. A. Cotton, L. Kruckzinski, B. Shapiro, and L. Johnson, *J. Am. Chem. Soc.*, **94**, 6191 (1972).
(45) B. Heaton, D. Toni, P. Chini, A. Fumagalli, D. McCaffrey, and S. Martinengo, *J. Chem. Soc., Chem. Commun.*, 523 (1975).
(46) F. A. Cotton and G. Wilkinson, "Advanced Inorganic Chemistry", 2nd ed, Interscience, New York, N.Y., 1975.
(47) The X-ray crystal structure of a rhodium-carbonyl cluster containing an encapsulated phosphorus atom is being determined and the results will be reported later.
(48) Other sulfur–rhodium–carbonyl clusters have been isolated by the reaction of $Rh_4(CO)_{12}$ with tetrahydrothiophene and other sulfur ligands under variable experimental conditions. (J. L. Vidal and Z. C. Mester).
(49) We have found that a total of 242 electrons are required by $[Rh_{17}(S)_2(CO)_{32}]^{3-}$ to satisfy the noble gas rule as calculated by $N_3 = 18N_i - 2N_2$.[1] Electron-counting for the anion results in 232 electrons = $(9 \times 17) + (2 \times 32) + (2 \times 6) + 3$, indicating this species is an exception to the rule. This conclusion has been reached by assuming that the encapsulated rhodium atom is equivalent to those on the surface. Applications of Wade's rules (*Adv. Inorg. Chem. Radiochem.*, **18**, 1 (1976)) in a manner similar to that reported by Chini et al., $N_3 = 14N_i + X$, results in a total of 226 electrons if the condensed square antiprismatic structure of the cluster is considered as a closo polyhedron ($N_1 = 16$): $(14 \times 16) + 2$.

On the N(7),O(6) Chelation Mode of 6-Oxopurines. Preparation and Structure of (*N*-Salicylidene-*N′,N′*-dimethylethylenediamine)(theophyllinato)copper(II)–3.5-Water

THOMAS J. KISTENMACHER,* DAVID J. SZALDA, CHIAN C. CHIANG, MIRIAM ROSSI, and LUIGI G. MARZILLI*

(*N*-Salicylidene-*N′,N′*-dimethylethylenediamine)(theophyllinato)copper(II)–3.5-water is orthorhombic, with $a = 12.570$ (4) Å, $b = 14.983$ (5) Å, $c = 23.249$ (8) Å, $V = 4378.6$ Å^3, $CuO_3N_6C_{18}H_{22}\cdot3.5H_2O$, $Z = 8$, $d_{measd} = 1.496$ (5) g cm^{-3}, and $d_{calcd} = 1.508$ g cm^{-3}. A model in space group *Pnna* has been refined by full-matrix least-squares techniques (nonhydrogen atoms anisotropic with the inclusion, but no refinement, of the hydrogen atoms associated with the complex) based on 3028 counter-collected F_o's to a final R index of 0.130 and a final weighted R index of 0.088. The waters of crystallization (hence the structure) appear to deviate slightly from space group *Pnna*. The primary coordination sphere about the copper is approximately square planar with the tridentate Schiff base and N(7) of the theophylline monoanion occupying the four coordination sites. Weak axial interactions involving O(6) of the theophylline monoanion and a water molecule are also observed. Crystal data are reported for the trihydrate and the monohydrate as well as the title compound.

Introduction

The title complex is a close analogue of (*N*-3,4-benzosalicylidene-*N′,N′*-dimethylethylenediamine)(theophyllinato)copper(II), I.[1] I is unique among 6-oxopurine complexes in

I
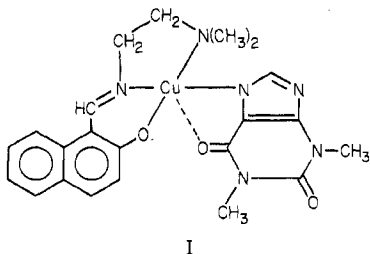
that in addition to the common metal–N(7) bond[1,2] a direct, *but weak*, bond is formed between the exocyclic oxygen atom at position 6 of the purine ring and an axial site on the Cu(II) center.[1]

Coordination of 6-oxopurines by such an N(7),O(6) chelation mode has been frequently postulated in the literature,[3] most recently[4–6] in connection with the mechanism of action of *cis*-Pt^{II}(NH$_3$)$_2$Cl$_2$, a wide-spectrum antineoplastic agent. Except for I, crystallographic studies of 6-oxopurine complexes have failed to reveal any direct interaction between O(6) and the metal.[1,2] Very frequently, the exocyclic oxygen O(6) interacts with hydrogen-bond donors either within the metal

complex or with other species in the crystalline lattice.[2,7] For example, in complexes analogous to I but containing only one methyl group (and hence one hydrogen atom) on the terminal nitrogen atom of the Schiff base ligand, O(6) does not interact with the Cu(II) but accepts a hydrogen bond from the terminal N–H group.[8,9]

In order to determine whether the weak N(7),O(6) chelate mode found in I would survive other crystalline environments, we have prepared and studied the crystal structure of the title complex.

Experimental Section

The complex (*N*-salicylidene-*N′,N′*-dimethylethylenediamine)-(theophyllinato)copper(II) was prepared in a very similar fashion to I.[1] Recrystallization from a variety of solvents yielded three crystalline hydrates: the monohydrate from 95% EtOH, the trihydrate from H$_2$O, and the 3.5 hydrate from MeOH.

Preliminary oscillation and Weissenberg photographs on all modifications gave crystal systems, rough cell constants, and space groups. Accurate cell dimensions and their associated standard deviations were obtained in each case from a least-squares fit of the setting angles for 15 reflections measured on a Syntex P1 automated diffractometer. Crystal densities were obtained by neutral buoyancy methods. Complete crystal data for all three hydrates are collected in Table I.

The 3.5 hydrate was chosen for a complete structural investigation as it formed crystals of the highest quality. A crystal with the following faces and mean dimensions was subsequently chosen for data collection: (010)–(0$\bar{1}$0), 0.27 mm; (100)–($\bar{1}$00), 0.16 mm; (001)–(00$\bar{1}$), 0.066